CEA/SACLAY
DSM

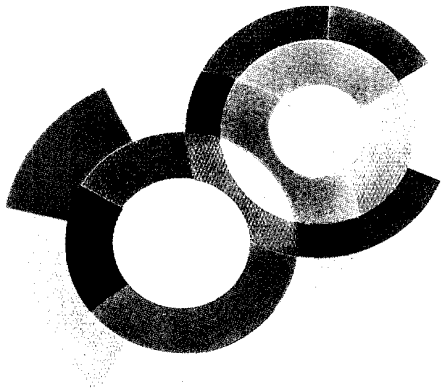

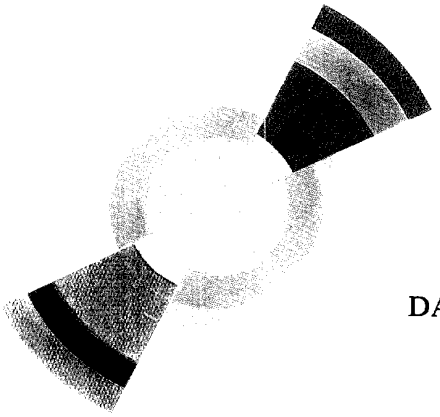

DAPNIA/SPhN-97-49 09/1997

Influence of the emission patterns on Li-Li azimuthal angular correlations in $^{36}Ar + ^{58}Ni$ dissipative collisions at 32 MeV/u

J. Benlliure, A. Chbihi, F. Saint-Laurent, J.P. Wieleczko, Ch.O. Bacri, E. Bisquer, B. Borderie, R. Bougault, R. Brou, J.L. Charvet, J. Colin, D. Durand, D. Cussol, R. Dayras, E. De Filippo, A. Demeyer, P. Ecomard, P. Eudes, D. Gourio, D. Guinet, P. Lautesse, J.L. Laville, L. Lebreton, C. Lebrun, J.F. Lecolley, A. Le Fèvre, R. Legrain, O. Lopez, M. Louvel, N. Marie, V. Métivier, L. Nalpas, A. Ouatizerga, J. Péter, E. Plagnol, A. Rahmani, T. Reposeur, M.F. Rivet, E. Rosato, S. Salou, M. Squalli, J.C. Steckmeyer, B. Tamain, L. Tassan-Got, O. Tirel, E. Vient, C. Volant

DAPNIA

Département d'**A**strophysique, de Physique des **P**articules, de Physique **N**ucléaire et de l'**I**nstrumentation **A**ssociée
CEA/Saclay F-91191 Gif-sur-Yvette Cédex

Submitted to Nuclear Physics A

Influence of the emission patterns on Li-Li azimuthal angular correlations in $^{36}Ar + ^{58}Ni$ dissipative collisions at 32 MeV/u. [1]

J. Benlliure [a,2], A. Chbihi [a], F. Saint-Laurent [a,3], J.P. Wieleczko [a], Ch.O. Bacri [b], E. Bisquer [e], B. Borderie [b], R. Bougault [d], R. Brou [d], J.L. Charvet [c], J. Colin [d], D. Durand [d], D. Cussol [d], R. Dayras [c], E. De Filippo [a,4], A. Demeyer [e], P. Ecomard [a], P. Eudes [f], D. Gourio [f,2], D. Guinet [e], P. Lautesse [e], J.L. Laville [f], L. Lebreton [e], C. Lebrun [d], J.F. Lecolley [d], A. Le Fèvre [a], R. Legrain [c], O. Lopez [d], M. Louvel [d], N. Marie [a,5], V. Métivier [d], L. Nalpas [c], A. Ouatizerga [b], J. Péter [d], E. Plagnol [b], A. Rahmani [f], T. Reposeur [f], M.F. Rivet [b], E. Rosato [d,6], S. Salou [a], M. Squalli [b], J.C. Steckmeyer [d], B. Tamain [d], L. Tassan-Got [b], O. Tirel [a], E. Vient [d], C. Volant [c].

[a] *GANIL, BP 5027, F-14076 Caen Cedex 5, France*

[b] *IPN Orsay, IN2P3-CNRS, 91406 Orsay Cedex, France*

[c] *CEA DAPNIA/SPhN, CE Saclay, 91191 Gif-sur-Yvette Cedex, France*

[d] *LPC, ISMRA, IN2P3-CNRS et Université, 14050 Caen Cedex, France*

[e] *IPN Lyon, IN2P3-CNRS et Université, 69622 Villeurbanne Cedex, France*

[f] *SUBATECH, IN2P3-CNRS et Université, 44072 Nantes Cedex, France*

Abstract

Fragment characteristics in Ar+Ni collisions at 32 MeV/u have been studied with the 4π array INDRA. The total detected charge in an event as well as the polar angles of the emitted fragments have been used to select dissipative collisions. Li-Li azimuthal angular correlations for such selection show strong anisotropies, resembling emission from a rotating source. However, a more refined impact parameter sorting based on kinematical analysis allows to show that the observed anisotropies are essentially due to the emission of fragments by two decaying sources identified as the partners of highly damped collisions. This statement is supported by a successful comparison of the data with statistical decay calculations assuming such a reaction scenario.

Preprint submitted to Elsevier Science *August 1, 1997*

PACS : 25.70.Pq

Keywords : NUCLEAR REACTIONS,^{58}Ni(^{36}Ar,X), E=32 MeV/u ; charged products detected with a 4π array ; dissipative collisions ; azimuthal angular correlations ; kinematical analysis ; Statistical model calculations.

1 Introduction

Highly dissipative nuclear reactions at intermediate bombarding energies can produce strongly excited nuclear matter. In this energy regime, numerous experiments have shown that the dominant decay channel is the so-called multifragmentation process, in which several intermediate mass fragments (IMF) with charge $Z \geq 3$ are emitted in a short time scale [1–3] (and references therein).

The understanding of this process is at the focus of many experimental investigations involving 4π detection arrays. Sophisticated techniques are developed to extract information about the multifragmentation mechanism(s). For example, fragment-fragment relative velocity and angular correlations have proved to be a very powerful tool to investigate the disintegration of excited nuclei. These techniques have been used to extract time scales, nuclear shapes and sizes, as well as the order of emission of the different fragments [3]. Such space-time characteristics together with the charge partition properties are essential to identify the exact mechanism(s) responsible for the multifragmentation process and to insure instructive comparison to the various theoretical approaches [4–9].

Up to now very few experimental studies have been dedicated to quantify the amount of angular momentum transferred to an eventual fusion source at intermediate energies [10]. This question has recently been addressed for a variety of entrance channels at bombarding energy around 30 MeV/u [11,12]. In these reactions, dissipative collisions have been selected by the detection of rare charged product pairs at large polar angles. The angular momentum

[1] Experiment performed at GANIL (DSM/CEA, IN2P3/CNRS)

[2] present address: GSI, Postfach 110552, 64220 Darmstadt, Germany

[3] present address: CEA,DRFC/STEP, CE Cadarache, 1308 Saint Paul lez Durance Cedex, France

[4] present address: INFN and Dipartimento di Fisica, Corso Italia 57, 95129 Catania, Italy

[5] present address: Texas A&M University,College Station, Texas 77843

[6] present address: Dipartimento di Science Fisiche, Uni. di Napoli, 80125 Napoli, Italy

transferred into the assumed incomplete fusion source has been studied by means of fragment-fragment azimuthal angular correlations. Simulations of sequential emission from a rotating source show that the strong experimental anisotropy of the angular correlations can be accounted for by a large angular momentum transferred to the source. For example, a maximum spin value of $130\hbar$ was inferred for the reaction Ar+Ag at 34 MeV/u [11].

On the other hand particle-particle or/and fragment-fragment azimuthal correlations have been also used to probe the centrality in heavy-ion collisions. For example, Phair et al. [13] show a strong increase of the anisotropy of the azimuthal correlations from central to peripheral collisions. This feature for non-central collisions could obviously not be interpreted as due to a large spin transferred into a single rotating source, but rather as an ordered motion reflecting the binary nature of the reaction mechanism. Since fusion-like processes and binary mechanisms can induce similar anisotropies, it is crucial to localize the frontier between both mechanisms. This is particulary important in light of numerous experimental studies [14–20] which have shown that for most collisions the mechanism is essentially binary with the formation of a quasi-projectile (QP) and quasi-target (QT) even for central collisions. Therefore, it is necessary to carry out simultaneously the analysis of the azimuthal correlations and the determination of the origin of the reaction products.

In this work we use the powerful capabilities of the multidetector INDRA to investigate the azimuthal angular correlations for lithium pairs, together with the study of the reaction mechanisms for the system Ar+Ni at 32 MeV/u. In the first step of the analysis the Li-Li azimuthal angular correlations are built for dissipative collisions selected by means of a criterion on the total charge detected in an event and fragment emission polar angle. Then we perform a more refined impact parameter sorting based on kinematical analysis. Finally we discuss the influence of the emission patterns on the anisotropy of the azimuthal correlations.

The paper is organized as follows: the experimental set-up is described in section 2. Section 3 is devoted to the event selection and the experimental azimuthal correlations. Data are analysed within two extreme assumptions: emission from a single source (section 4) offering an extraction of the spin; and emission from a QP and QT system (section 5) using kinematical analysis. A summary and conclusions are given in section 6.

2 Experiment set-up description

The experiment was performed using the multidetector INDRA [21,22]. The primary 37 MeV/u ^{36}Ar beam delivered by the GANIL facility was slowed

down to 32 MeV/u. After magnetic analysis by the GANIL "Alpha spectrometer", the ^{36}Ar projectiles impinged onto a ^{58}Ni target, 193 $\mu g/cm^2$ thick. The beam intensity was $3 - 4.10^7 pps$.

The multidetector INDRA covers about 90% of the 4π solid angle. The total number of detection cells is 336 arranged according to 17 rings centered on the beam axis. The first ring (2°-3°) is made of fast NE102/NE115 phoswich detectors. The rings 2 to 9 cover the angular range from 3° to 45° and are made of three detection layers : a low pressure gas-ionization chamber, a 300 μm thick silicon detector and a 14 to 10 cm thick CsI(Tl) scintillator. The remaining 8 rings cover the angular range from 45° to 176° and have two detection layers : ionization chamber and 7.6 to 5 cm thick CsI(Tl) scintillator. For the studied system Ar + Ni, fragments with Z up to 34 (the total initial charge is 46) are identified in the forward region. Beyond 45°, the ion identification is obtained up to Z=16. Over the whole angular range, a very good isotope identification is obtained for Z=1 to Z=3, except for particles with low energies where ambiguities are unresolved.

The energy calibration of the CsI(Tl) scintillators was obtained for light charged particles (LCP) by means of the elastic and inelastic scattering of secondary LCP beams ($p, d, t, ^3He, ^4He$) produced by the fragmentation of a 95 MeV/u ^{16}O beam in a thick C target. These particles were then momentum selected by the "alpha magnetic spectrometer" and scattered from a C or Ta target installed in the INDRA reaction chamber. For $Z \geq 3$ fragments, the energy calibration was made by using the ΔE/E technique. The energy resolution was about 4%. The energy threshold was a few 100 keV for light particles, 0.7 MeV/u for Z=3 and 1.4 MeV/u for Z=35. A complete technical description of INDRA, its calibration and its electronics can be found in [21,22].

The Li-Li azimuthal angular correlations were constructed for particles emitted between the polar laboratory angles 14° and 70°. The detectors in this angular range belong to rings 6 to 11 with intervals in polar angles of $6.0° \leq \Delta\theta \leq 13°$. The nearest neighbor azimuthal spacing in this region of INDRA is $\Delta\phi$=15°. Table 1 gives more details concerning the segmentation over the whole angular range. This segmentation of INDRA makes possible the investigation of the fragment-fragment azimuthal angular correlations.

For all data reported in this paper, events were recorded with the requirement that 3 or more modules fired in each event. However, a minimum bias trigger (multiplicity greater than zero) was also used for normalization purpose. A comparison between the two sets of data shows no influence of the trigger on the class of events discussed in the present work.

3 Event selection and experimental azimuthal correlations

3.1 Event selection

The total multiplicity distributions for the identified charged products (Z$\geq$ 1), N_c, is shown in fig. 1a (white area). This distribution exhibits a well-known shape with a bump at high multiplicity which is associated to the most dissipative processes in the reaction. The data obtained with the minimum bias trigger gives the same shape of the N_c distribution except for low values ($N_c \leq 3$) where the yield is much higher than the one shown in fig. 1a. This confirms that the triggering condition (3 or more modules fired) eliminates only very peripheral collisions which are not studied in this paper.

The total detected charge (Z_{tot}) in an event is shown in fig. 1b as a function of the multiplicity N_c. Three domains are visible: a component with small values for both Z_{tot} and N_c corresponding to the events where neither the projectile-like nor the target-like remnants are detected; a component starting at Z_{tot}=18 associated to peripheral collisions where the projectile-like fragment is collected, but not the target-like residue; last, a wide zone located around Z_{tot}=40 and N_c=14 which corresponds to events where a large part of the total available charge of the system ($Z_1 + Z_2 = 46$) is collected and identified.

In this work we have kept only events in which the total detected charge Z_{tot} exceeds 35 *i.e.* 76% of the total available charge (a condition indicated by the horizontal line on fig. 1b). Figure 1a (grey area) shows the total multiplicity distribution for those events. It is clear that the largest multiplicities have been selected and thus the most dissipative collisions in the reaction. The dark area in fig. 1a represents the multiplicity distribution where, in addition to the above selection on Z_{tot}, at least two lithiums are detected between 14^o and 70^o in the laboratory frame. The distribution for these events is peaked around N_c=15 which indicates a large energy deposition.

Our selection is similar to the one used in [11]. Indeed, the emission angle window for each lithium is chosen to minimize possible contributions from pre-equilibrium and QP emission. In doing so, it was expected that collisions leading to an incomplete fusion system could be isolated. The last assumption will be discussed later by means of kinematical analysis. Another reason to keep only large angles is the fact that, regardless of the reaction mechanism, the reaction plane is perpendicular to the relative angular momentum, whose direction is poorly defined for emission close to the beam axis, while a better characterization is obtained at larger emission angles.

3.2 *Experimental azimuthal correlations*

Angular correlations for relative azimuthal angle ($\Delta\phi$) were extracted event by event for the Li-Li pairs. We have checked that the $\Delta\phi$ distributions for mixed events are flat, which gives confidence that correlations for real coincidences are not affected by the detector efficiency. The choice of lithium pairs is due to the well known experimental fact that,the heavier the emitted particle, the stronger is the anisotropy.

The normalized azimuthal angular correlations C($\Delta\phi$) for the Li-Li pairs detected between $\theta = 14^o$ and $\theta = 70^o$ in the laboratory frame are shown in figure 2. The normalization is given by the total number of counts divided by the number of angular bins. The pairs detected at the same laboratory polar angle were excluded for two reasons. The first one is for a normalization purpose. The number of possible combinations between two lithiums detected in the same ring (same polar angle) is different from the number of possible combinations of the Li pairs coming from two different rings (for example, 23 possible combinations for a same ring 4, and 24 possible combinations for ring 4 and 5). The second reason is that the shape of the correlations at small azimuthal angles, is sensitive to the average time between successive emissions. Thus taking into account emission at the same polar angle would significantly affect the behaviour of the azimuthal correlations around $\Delta\phi = 0^o$ (this relative angle is not allowed in the same ring). Since our investigations do not address the topic of fragment emission time, we may have included emission at the same polar angle, but we preferred to stick as close as possible to the analysis presented elsewhere [11,12].

Several features can be extracted from figure 2. When the two lithiums are emitted on the opposite side with respect to the beam axis, we observe a strong anisotropy defined as the ratio $C(\Delta\phi = 180^o)/C(\Delta\phi = 90^o)$. We can also see a clear same side/opposite side asymmetry with a depletion for $\Delta\phi \approx 0^o$. The same features have been observed in the reaction ^{40}Ar + $^{Nat.}$Cu at 34 MeV/u [11], an entrance channel close to our system. Two possible interpretations can be given to explain the shape of this azimuthal correlation. The first one is based on the assumption that a single source is formed and the anisotropy is essentially an angular momentum effect. The second interpretation assumes that the collision leads to two-body emitting sources. In this case the anisotropy is due to the reaction dynamics.

4 A single source assumption

4.1 Experimental features

In the single source scenario one assumes that the projectile and target nuclei partially fuse and form a hot rotating compound like nucleus which deexcites statistically. In the statistical model the angular distribution of the emitted particles is given by the relation:

$$W(\psi) \propto exp(\beta sin^2\psi) \tag{1}$$

where ψ is the emission angle with respect to the direction of the emitter angular momentum. This distribution depends on the magnitude of the β parameter defined as:

$$\beta = J_o^2\hbar^2/2TI_{eff} \tag{2}$$

which increases with the angular momentum of the emitter, J_o, and decreases with the temperature, T. I_{eff} is the effective moment of inertia.

Within this scenario, the strong anisotropy observed in fig. 2 is a signature of a rotational collective motion of the emitter, with a high angular momentum transferred to the source. This in turn favours particle emission in a plane perpendicular to the spin. Moreover, the same side/opposite side asymmetry of the angular correlations reflects the recoil effect of the source due to momentum conservation, the influence of which is expected to be more important for such a light system. The low yield for $\Delta\phi \approx 0°$ may indicate a final state Coulomb interaction due to the short delay time between the emission of fragments [11].

4.2 Statistical calculations assuming a single emitter

In order to understand quantitatively these effects we have performed simulations with the event generator GENEVE [23]. The decay of the emitter is simulated within the framework of the statistical model which assumes sequential emission. The modelization of the decay process is similar to the one used in the statistical code GEMINI [24]. In our calculations we use $a = A/13$ for the level density parameter. The characteristics of the source ($A_s = 85$, $Z_s = 42$, $E^* = 400$ MeV and $V_s = 2.5$ cm/ns, respectively, the mass, charge, excitation energy and velocity in the laboratory frame) were chosen according to the systematics of linear momentum transfer [25] and from results of

the Boltzmann-Uehling-Uhlenbeck (BUU) calculations for a similar system (Ca+Ca at 35 MeV/u) [26].

Extensive simulations have been performed to fit the anisotropy $C(\Delta\phi = 180°)/ C(\Delta\phi = 90°)$. This quantity depends mainly on the magnitude of the spin of the emitter and the other parameters have a lesser influence. The simulated events were filtered through the experimental device and analysed like the data. The results of two calculations are compared to the data in figure 2. The dashed line represents the result when a single angular momentum value of $60\hbar$ is assumed. One observes that the anisotropy ratio, $C(\Delta\phi = 180°)/C(\Delta\phi = 90°)$, is not strong enough. A calculation assuming a single value of $100\hbar$ (full line) gives a better agreement for the whole azimuthal angular range, although the yield for the same side emission is overestimated. Both calculations indicate an asymmetry same side/opposite side which is interpreted as recoil effects of the emitter. As it is difficult to handle the shape of the spin distribution, these spin values must be taken as mean values. Finally, the calculations do not show the depletion at $\Delta\phi = 0°$, since the time delay between successive emission is not explicitly included in the model. Indeed, within the scenario of statistical emission from a hot nucleus, the depletion of the correlation at small angles can be explained by the final state Coulomb repulsion due to a short time delay between the two Li emissions. These effects have been already studied by the Stony Brook group for ^{40}Ar induced reactions [11]. A time delay of the order of $10^{-22}s$ between successive emissions of Li fragment was deduced from their work.

To summarize this first step of the analysis, one can conclude that the strong anisotropy of the azimuthal angular correlations can be accounted for by a large angular momentum transferred to a fusion-like source. The key hypothesis of such analysis is that the lithiums originate from a class of events selected through polar angle emission. This is examined in the next section.

5 Two-body source assumption

5.1 Event selection using global variables

To gain more insight on the origin of the reaction products, we have performed an analysis based on global variables taking into account the kinematical characteristics of the fragments produced in the reaction. Previous works [27] have shown that the second moment of Fox and Wolfram [28] is well suited to select

the most central collisions. This observable is defined as:

$$H(2) = \frac{1}{H(0)} \sum_{i,j}^{M_{IMF}} |\vec{p_i}||\vec{p_j}| \frac{(3cos^2\theta_{ij} - 1)}{2} \tag{3}$$

$$H(0) = \sum_{i,j}^{M_{IMF}} |\vec{p_i}||\vec{p_j}| \tag{4}$$

where p_i is the momentum of fragment i calculated in the center of mass (c.m) of the event, and θ_{ij} is the relative angle between fragments i and j, expressed also in the c.m. This variable provides a measure of event shapes in momentum space. For ideal cases an isotropic source is characterized by H(2) close to 0, while for two well separated sources H(2) is close to 1.

Figure 3 shows the H(2) distribution obtained for the events in which $Z_{tot} \geq 35$ and two Li's are detected in the whole angular range (in order to improve the statistics, no restriction has been made on the detection angles of the two Li's). We observe that these events cover a wide range in H(2) corresponding to events with different shapes in momentum space. It is worth noting that due to the influence of the finite number of the emitted products, fluctuations lead also to a large distribution of this observable [29], even for an isotropic source.

In order to illustrate the selection produced by the observable H(2), we have plotted in figure 4 (left panels), the invariant velocity diagrams ($V_{||}$-$V_{\perp}$) of the emitted ^4He particles for events with four different bins in H(2) values. Clearly, events with large H(2) values present two emission sources. Furthermore, the relative velocity between them decreases with H(2). Only for very small H(2) the events could be attributed to a single source or two close sources. This behaviour reflects the increase of the centrality of the collision as H(2) decreases. In the same figure (right panels), we show the azimuthal angular correlations built for Li pairs emitted in the whole angular range and for the same bins in H(2). The anisotropy changes dramatically with the centrality of the collisions. For the smallest H(2) value the anisotropy vanishes whereas it is strongly enhanced for large H(2) values. The same features are observed when we apply the selection on the polar angles between $\theta = 14°$ and $\theta = 70°$ (not shown here). These results indicate a clear influence of the emission patterns on the shape of the azimuthal correlations.

The ^4He velocity diagrams (left panels on fig.4) for large values of H(2) ($\geq$ 0.4) show two components. These features can be interpreted in terms of binary dissipative collisions or fission of a single rotating source. To distinguish between these two possible interpretations, we have extracted the average parallel velocity of the largest fragment ($\bar{V}_{//}^{LF}$). For $H(2) \leq 0.2$, we found out

that $\bar{V}_{//}^{LF}$ is close to zero in the c.m frame and for $H(2) \geq 0.3$ the largest fragment in the event has a negative c.m velocity, close to the target c.m velocity. This is a good indication that in the last case we are not dealing with fission of a single source but rather with the target remnant of a binary collision.

From the above analysis one can conclude that for ^{36}Ar + ^{58}Ni at 32 MeV/u, binary dissipative collisions are the dominant process leading to emission of lithiums. This agrees with the analysis of the same data [30] using a less restrictive class of events. Only for $H(2) \leq 0.2$, could the events be possibly attributed to a single source. On the other hand, the associated correlation (fig. 4 right panel top) reveals no anisotropy and then no evidence of high spin is found.

5.2 Separation of the two sources using the thrust technique

The events associated to large H(2) values ($H(2) \geq 0.3$) were analysed in terms of binary deep-inelastic collisions. This was done event by event using the thrust technique [31], with the aim of identifying products emitted by the primary partners of the reaction as in reference [32,30]. The detected fragments are partitioned into two families C_1 and C_2 and one searches for the partition maximizing the thrust defined as:

$$T_2 = \frac{|\sum_{i \in C_1} p_i| + |\sum_{j \in C_2} p_j|}{\sum_{k \in C_1, C_2} |p_k|} \tag{5}$$

The maximum T_2 value corresponds to the situation for which the two groups of particles are the most separated in the momentum space.

The reconstructed charge of the primary partners are shown in figures 5a and 5b. As it can be seen the mean charges obtained are $Z_{QP} \approx 17$ and $Z_{QT} \approx 25$. These values are close to the charge of the projectile (Z=18) and target (Z=28), respectively. The bigger charge loss of the target can be understood by taking into account the detection thresholds which affect mainly products from the QT, whereas the geometrical detection efficiency (90%) affects both QP and QT products. The thrust technique provides also the center of mass velocity of the decaying nuclei and relative velocity v_R between them. The energy dissipated in the collisions has been calculated according to the expression [33]:

$$E^* = E_{CM} - \frac{1}{2}\mu v_R^2 \tag{6}$$

where μ is the reduced mass of the initial system and E_{CM} is the available c.m. energy. Figures 5c and 5d show the relative velocity and dissipated energy distributions obtained for the binary reactions ($H(2) \geq 0.3$). The mean relative velocity obtained is $\bar{v}_R \approx 4.7 cm/ns$ and the mean dissipated energy is $\bar{E}^* \approx 5 MeV/u$.

Once this characterization procedure of the primary partners is achieved, the Li-Li azimuthal angular correlations are built for each reconstructed partner. The whole azimuthal angular correlation obtained for the binary collisions is presented in figure 6a. Figure 6b (respectively fig. 6c) corresponds to the azimuthal correlation constructed with Li pairs emitted by the QP or forward source (QT or backward source). Finally in figure 6d we represent the azimuthal correlation when one Li is emitted by the QP and the other one by the QT. This analysis allows to better understand the different correlation functions shown in fig. 4 (right panels) as a function of H(2). For large H(2), the large relative velocity between the two sources (QP and QT) enhances the correlation of particles coming from same source (both lithiums are emitted either by the QP or by QT). The relative velocity decreases for smaller H(2) values and then the correlation due to lithiums coming from the different sources (one lithium emitted by the QP and the other by the QT) becomes more important.

5.3 Statistical calculations assuming two emitting sources

Simulations assuming two independent sources decaying statistically have been performed to check if such a scenario can induce the strong anisotropy observed experimentally. To do so, the event generator GENEVE [23] is used to describe the deexcitation of both partners. The mean relative velocity between both sources and their average sizes are taken from the data. The excitation energy of the QP and QT is calculated from the experimental total dissipated energy, shared according to the ratio of their masses. This sharing has been widely observed at low bombarding energies (around 10 MeV/u) and even at 27 MeV/u [34]. Whether this characteristic is still present for our system (at 32 MeV/u) is an open question. Indeed recent results obtained for the same system Ar+Ni but at 52 MeV/u [30], indicate some departure from low bombarding energy regime. Nevertheless our conclusions will not depend strongly on the exact sharing of the excitation energy. Finally, $10\hbar$ (resp. $15\hbar$) has been assumed for the intrinsic spin of the QP (resp. QT). These values have to be taken as indicative but they are comparable to a simple estimate assuming a sticking between both partners at an impact parameter of 3 fm ($7\hbar$ for QP and $16\hbar$ for QT).

The filtered results of the calculations are compared to the data obtained for

the binary events in figure 6. In this figure the lines represent the azimuthal angular correlations calculated in the same way as it was done for the data. Reasonable agreement is observed for all cases. The results of these calculations confirm our interpretation that events with large H(2) values correspond to binary collisions and the strong anisotropy that we observe in the azimuthal angular correlations is induced by the binary character of the collisions.

6 Summary and conclusions.

Li-Li azimuthal angular correlations have been investigated for the most dissipative collisions in the reaction Ar+Ni at 32 MeV/u. A first selection of these dissipative collisions by charged particle multiplicity criterion produces a strong anisotropy in the correlations. Within the framework of a statistical deexcitation of a single rotating source, the anisotropy could be associated with high spin values (60 to 100$\hbar$), as pointed out by other authors [11,12].

The high selection capabilities of the INDRA detector allowed a better determination of the most central collisions. By using a kinematical analysis of the emitted particles we show that the first selection criterion was not accurate enough to select events where a possible single rotating source is formed. In fact we demonstrate that the observed anisotropy in the azimuthal correlations is induced by kinematical recoil effects between the QP and the QT in binary collisions. The study of the events where a possible single rotating source is formed reveals no anisotropy in the azimuthal correlation and then no evidence of high spin values is found, at least within the framework of the statistical model that we use. Further studies can provide information about the emission times of the IMF's from the final state interaction and hence about the sequential or prompt character of the emission.

Another important conclusion related to the study of the deexcitation mechanism of hot nuclei formed in intermediate energy collisions is the predominance of deeply inelastic collisions. This binary character of the reaction can produce spurious correlations induced by the presence of a QP and a QT and make questionable the analysis in terms of 'thermal scaling' [35] as well as the extraction of high spin values. Such analysis require a careful identification and characterization of the decaying source(s).

7 Acknowledgments

We thank the staff of the GANIL Accelerator facility for their support during the experiment. This work was supported by the Commissariat à l'Energie

Atomique, Centre National de la Recherche Scientifique, le Ministère de l'Education Nationale et le Conseil Régional de Basse-Normandie.

References

[1] W. G. Lynch, Ann. Rev. Nuc. Sci. 37 (1987) 493.

[2] L. Moretto, G. Wozniak, Ann. Rev. Nuc. Sci. 43 (1993) 379.

[3] B. Tamain, D. Durand, Preprint LPCC 97.16
(to be published in Proceedings of the Summer School Les Houches ed. H. Nifenecker (1997)).

[4] J.P. Bondorf et al., Nucl. Phys. **A443** (1985) 321.

[5] D.H.E. Gross, Rep. Prog. Phys. **53** (1990) 605.

[6] W.A. Friedman, Phys. Rev. Lett. **60** (1988) 2125 and Phys. Rev. **C42** (1990) 667.

[7] E. Suraud et al., Phys. Lett. **B229** (1989) 359.

[8] Ph. Chomaz et al., Phys. Lett. **B254** (1991) 340.

[9] G.F. Burggio et al., Phys. Rev. Lett. **69** (1992) 1888.

[10] M.N Namboodiri et al., Phys. Rev. **C35** (19987) 149.

[11] T. Ethvignot et al., Phys. Rev. **C48** (1993) 618.

[12] D. Benchekroun et al., Z. Phys. **A356** (1997) 411.

[13] L. Phair et al., Nucl. Phys. **A564** (1993) 453.

[14] J. Péter et al., Nucl. Phys. **A593** (1995) 95.

[15] J.C. Steckmeyer et al., Phys. Rev. Lett. **76** (1996) 4895.

[16] R. Bougault et al., Nucl. Phys. **A587** (1995) 499.

[17] V. Métivier et al., Proc. of the ACS Nucl Chem. Symp., Anaheim, CA, April 1995.

[18] R. Dayras et al., Phys. Rev. Lett. **62** (1989) 1017.

[19] B. Borderie et al., Phys. Lett. **B205** (1988) 26.

[20] M.F Rivet et al., XXXI International Winter Meeting on Nuclear Physics, Bormio, Italy, January 1993, Proceedings edited by I. Iori, Ricerca Scientifica ed Educazione Permanente Suppl. N.97, p. 323.

[21] J. Pouthas et al., Nucl. Inst. and Meth. **A357** (1995) 418.

[22] J. Pouthas et al., Nucl. Inst. and Meth. **A369** (1996) 222.

[23] J.P.Wieleczko et al, Proc. II TAPS Workshop, Guardamar, Spain 1993, ed. J.diaz, G. Martinez, Y. Schutz,World Scientific, p. 145.

[24] R.J. Charity et al., Nucl. Phys. **A483** (1988) 371.

[25] H. Morgenstern et al., Phys. Rev. Lett. **52** (1984) 1104.

[26] K. Hagel et al., Phys. Rev. Lett. **68** (1992) 2141.

[27] N. Marie, thesis Université de Caen 1996, unpublished.

[28] G.C. Fox and S. Wolfram, Phys. Rev. Lett. **41** (1978) 1581.

[29] J.D. Frankland et al., XXXV International Winter Meeting on Nuclear Physics, Bormio, Italy, February 1997, Proceedings edited by I. Iori, Ricerca Scientifica ed Educazione Permanente Suppl. N.110, p. 323.

[30] J.L. Charvet et al., XXXV International Winter Meeting on Nuclear Physics, Bormio, Italy, February 1997, Proceedings edited by I. Iori, Ricerca Scientifica ed Educazione Permanente Suppl. N.110, p. 309.

[31] J. Cugnon and D. L'Hote, Nucl. Phys. **A397** (1983) 519.

[32] E. de Filippo et al., XXXIII International Winter Meeting on Nuclear Physics, Bormio, Italy, January 1995, Proceedings edited by I. Iori, Ricerca Scientifica ed Educazione Permanente Suppl. N.101, p. 217.

[33] D. Durand et al., Phys. Lett. **B345** (1995) 397.

[34] B. Borderie et al., Z. Phys. **A338** (1991) 369.

[35] L.Phair et al., Phys. Rev. Lett. **77** (1996) 822.

Segmentation of the INDRA detectors				
Ring number	$\bar{\theta}^o$	$\Delta\theta^o$	$\Delta\phi^o$	$\Delta\Omega(msr)$
1	2.5	1.0	30	0.37
2	3.8	1.5	30	0.74
3	5.6	2.5	15	1.01
4	8.4	3.0	15	1.70
5	11.7	4.0	15	3.21
6	16.9	6.0	15	7.01
7	23.0	7.0	15	11.17
8	30.9	8.0	15	15.79
9	39.4	10.0	15	26.43
10	50.6	12.0	15	39.60
11	63.0	13.0	15	50.31
12	79.3	18.0	15	77.50
13	101.0	18.0	15	80.07
14	119.1	16.0	22.5	93.50
15	135.0	16.0	22.5	73.06
16	149.8	15.0	45	91.19
17	166.4	19.0	45	50.89

Table 1
$\bar{\theta}^o$: average polar angle, $\Delta\theta^o$: opening polar angle, $\Delta\phi^o$: opening azimuthal angle and $\Delta\Omega(msr)$: solid angle.

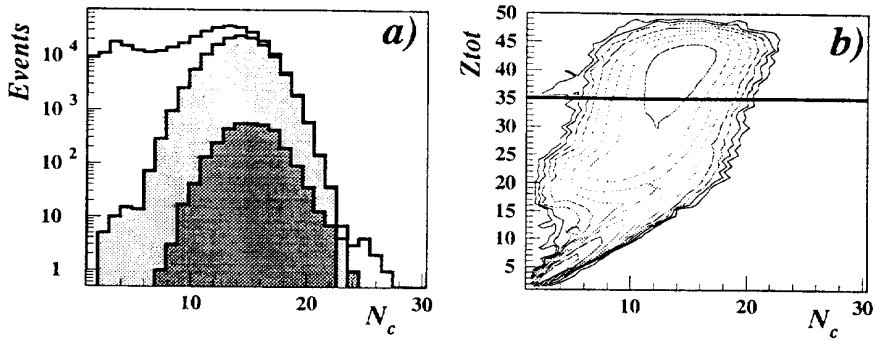

Fig. 1. *Total multiplicity distributions of charged products: (a) for all events (white area); for events having a total detected charge $Z_{tot} \geq 35$ (grey area); for events having a total detected charge $Z_{tot} \geq 35$ and at least two Li's detected between $\theta = 14^o$ and $\theta = 70^o$ in the laboratory frame (black area). (b) Total detected charge vs the charged product multiplicity; the horizontal line represents the cut $Z_{tot} = 35$.*

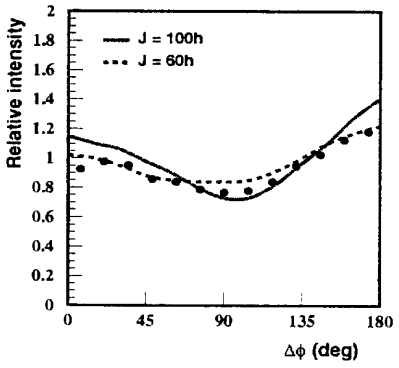

Fig. 2. *Azimuthal angular correlations between Li pairs detected in the angular laboratory range 14^o -- 70^o for events with $Z_{tot} \geq 35$. Solid points are the data, full and dashed lines correspond to statistical model calculations assuming the decay of a fusion-like source with single angular momentum values of 100ħ and 60ħ, respectively.*

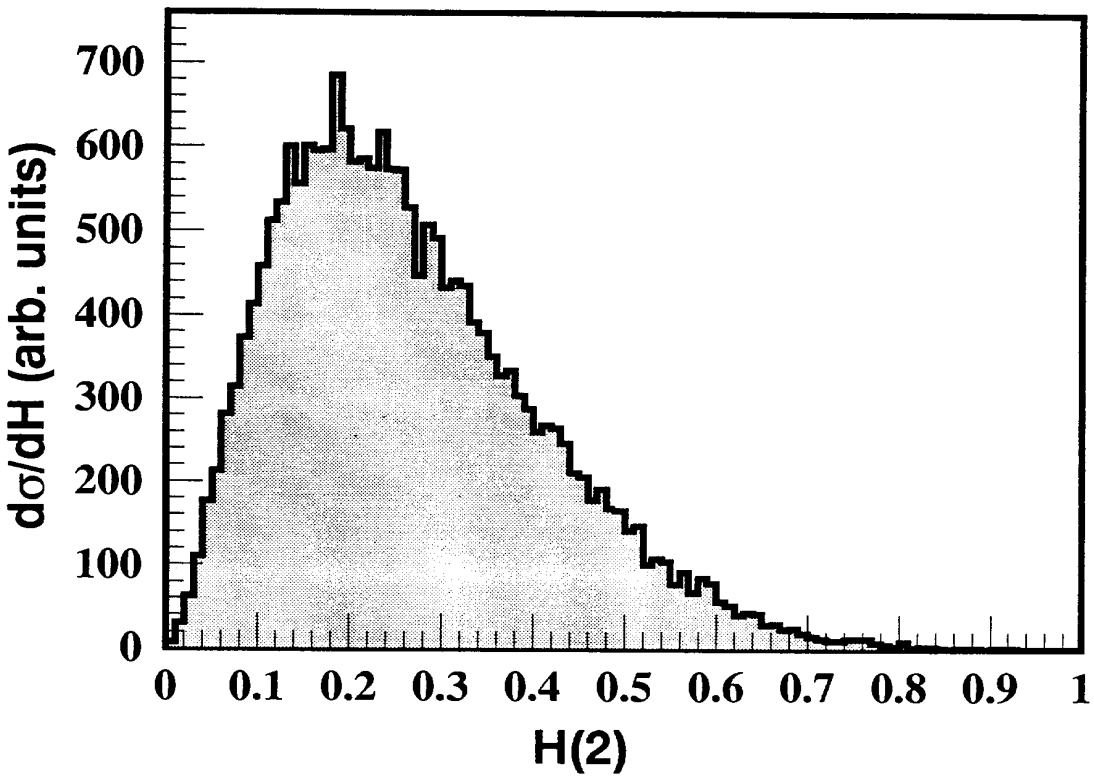

Fig. 3. *Distribution of the kinematical observable H(2), for events having* $Z_{tot} \geq 35$ *and at least two Li's emitted in the whole angular range (see text).*

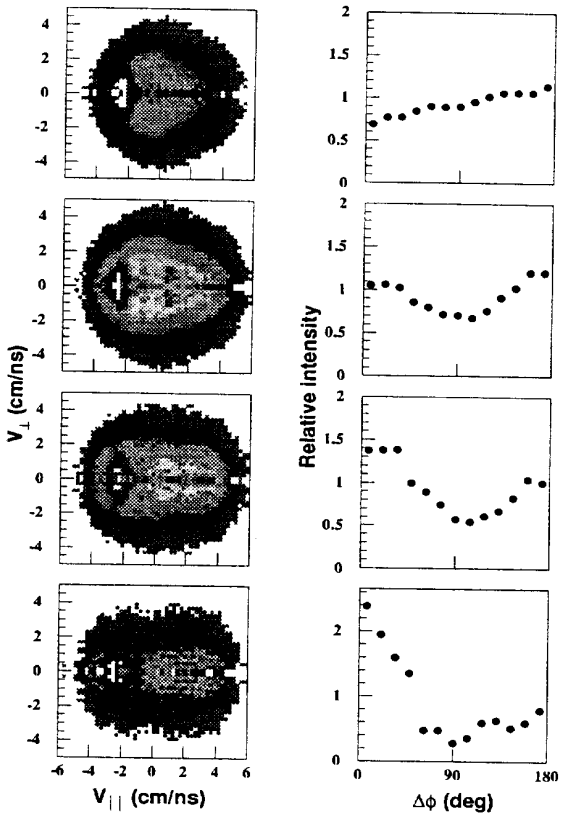

Fig. 4. *^4He $V_{||}$-$V_\perp$ plots and the corresponding azimuthal angular correlations of lithium pairs for four H(2) bins of* 0.2 *unit steps: starting from* $H(2) = 0. - 0.2$ *(top), to* $H(2) = 0.6 - 0.8$ *(bottom).*

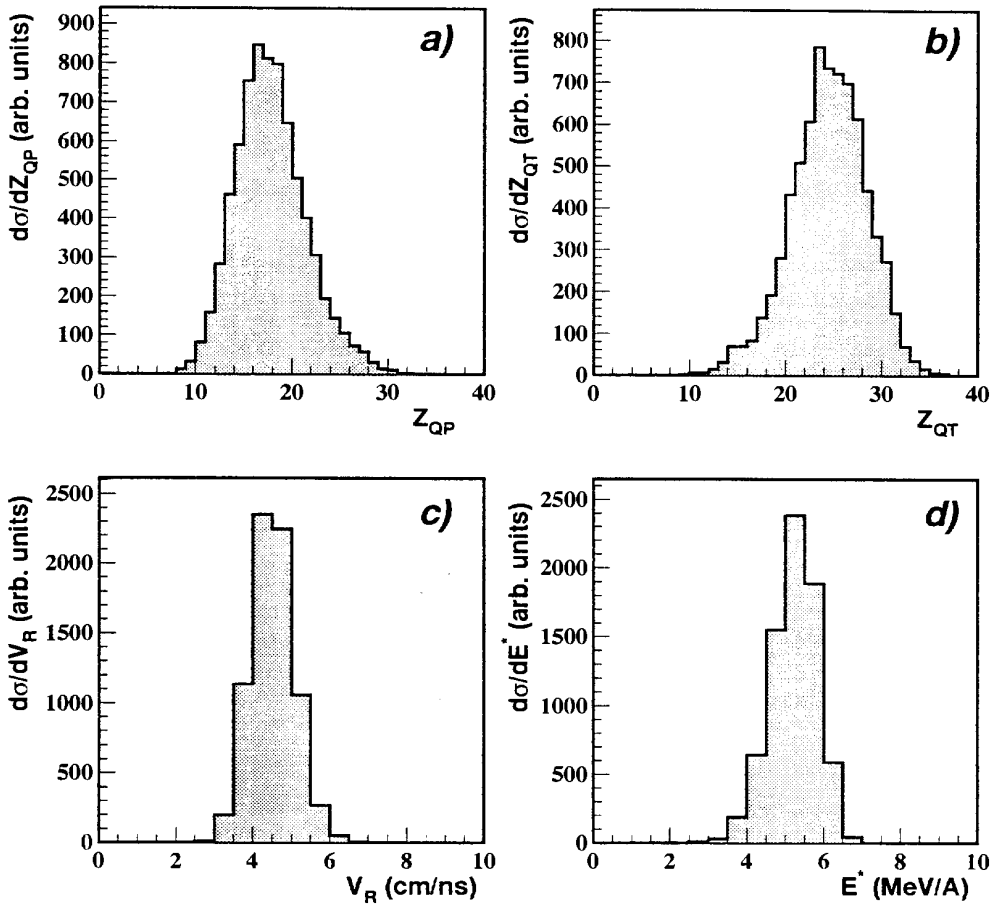

Fig. 5. *Characteristics of the two primary sources reconstructed with the thrust method (see text) for binary events ($H(2) \geq 0.3$). a) Reconstructed charge distribution of the QP. b) Reconstructed charge distribution of the QT. c) Relative velocity between the two primary sources. d) Distribution of the dissipated energy.*

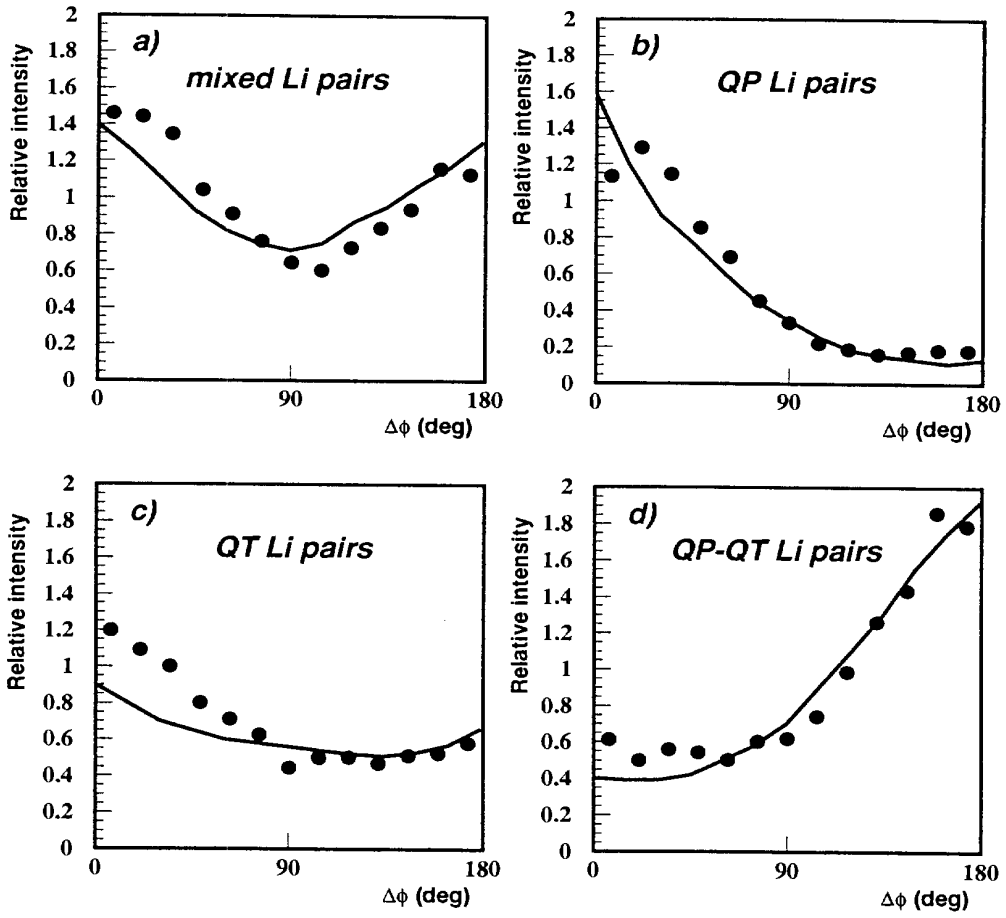

Fig. 6. *Azimuthal angular correlations between Li pairs for binary events ($H(2) \geq 0.3$) taking into account the emitting sources. The lines correspond to simulations with a statistical code (see text). a) Li pairs regardless of the origin. b) Li pairs come from the QP. c) Li pairs come from the QT. d) One Li comes from the QP and the other one from the QT.*